J Mater Sci (2010) 45:6206–6211
DOI 10.1007/s10853-010-4714-y

Oxygen partial pressure dependence of the properties of MgZnO thin films during annealing

W. W. Liu · B. Yao · Y. F. Li · B. H. Li · Z. Z. Zhang · C. X. Shan · J. Y. Zhang · D. Z. Shen · X. W. Fan

Received: 11 April 2010 / Accepted: 11 June 2010 / Published online: 24 June 2010
© Springer Science+Business Media, LLC 2010

Abstract Undoped n-type MgZnO films were deposited on *c*-plane sapphire substrates by molecular-beam epitaxy and subsequently annealed in O_2 at different pressures. After annealing at 3.03×10^5 Pa, oxygen content in the annealed films show increases and the films transform into p-type conduction. However, the decreases of oxygen content and the increases of electron concentration were obtained while the films annealed at 1.01×10^5 Pa or 2.05×10^{-3} Pa. The changes in intensity of the emission peak located at 2.270 eV are similar to the changes of the oxygen content in the films annealed at different pressures. According to the defect levels and the relationship between photoluminescence spectra and annealing condition, it was suggested that this emission peak was related to interstitial oxygen (O_i). The obtained p-type conduction is attributed to that the O_i acceptor can compensate oxygen vacancy and interstitial zinc donor.

Introduction

Due to its wide band gap and large exciton binding energy of 60 meV, zinc oxide (ZnO) based oxide semiconductors are strong candidate for gas sensors, thin-film transistors, surface acoustic wave devices, transparent electrodes for thin-film solar cells, and blue or ultraviolet light emitting diode (LED), and lasers diode (LD) [1–10]. For fabricating a double heterostructure laser diode using a ZnO active layer, two critical challenges are p-type doping and band gap engineering in alloy semiconductors. Since band gap of MgZnO alloy with wurtzite structure is larger than that of the ZnO and can be tuned by changing Mg content, it is considered as candidate barrier material for the ZnO based heterostructure [11–15].

However, this material has largely failed to live up to its potential, because LED and LD require both high quality n-type and p-type MgZnO, and it has been proven to be very difficult to produce a stable and reproducible p-type MgZnO with high conductivity and mobility. Minegishi et al. [16] obtained a p-type ZnO layer in 1997 through nitrogen doping. After this development, N, P, Sb, Li doping, intrinsic doping (by tuning oxygen pressure or Mg concentration in the growth environment), and co-doping of N with group-III elements have also resulted in p-type MgZnO films [17–23]. However, it is ambiguous for p-type doping mechanism and the stability as well as reproducibility of the p-type conduction in MgZnO films is a main issue at present in this research field. Therefore, it is worthwhile to investigate the intrinsic p-type behavior of MgZnO thin films before adopting any doping method.

There have been a few reports on undoped p-type ZnO and MgZnO films. Xiong et al. reported that the conductivity of ZnO films could depend on Ar/oxygen gas ratio during reactive sputtering. Zeng et al. as well as Choopun et al. produced intrinsic p-type conduction film by tuning the oxygen partial pressure [24–27]. In all the above, the oxygen contents or partial pressures were optimized during the O-rich growing process. Recently, Li et al. [22]

W. W. Liu · B. Yao (✉) · Y. F. Li · B. H. Li · Z. Z. Zhang · C. X. Shan · J. Y. Zhang · D. Z. Shen · X. W. Fan
Key Laboratory of Excited State Processes, Chinese Academy of Sciences, No. 16, Dong Nanhu Road, Changchun 130033, China
e-mail: yaobin196226@yahoo.com.cn

W. W. Liu
e-mail: wwliu_ciomp@126.com

W. W. Liu · Y. F. Li
Graduate School of the Chinese Academy of Science, Beijing 100049, China

reported that the intrinsic p-type MgZnO films can be obtained by controlling Mg content.

In this letter, undoped n-type MgZnO films were investigated by annealing at different pressures and p-type MgZnO films were obtained by post-annealing at 3.03×10^5 Pa in oxygen ambient. Effects of annealing pressure on the properties of the undoped MgZnO films and the mechanism of formation of the p-type conduction were discussed in the present work.

Experimental procedure

Undoped MgZnO films were grown on *c*-plane sapphire substrates by a V80H molecular-beam epitaxy (MBE) system equipped with double zone effusion cells, which are used for evaporating 6N Zn and 6N Mg metal sources. Before growing, the background pressure was 1.3×10^{-7} Pa. A RF-plasma source is used to produce reactive oxygen radicals. 5N oxygen gas is injected into the RF-plasma source through a mass flow controller system. The oxygen gas flow rate was kept at 1.0 sccm. The films were grown at 650 °C in the growth pressure of 1.6×10^{-6} Pa. After growing, the sample was cut into several pieces, and then annealed for 1 h at 600 °C in oxygen under three different annealing pressures. The annealing pressures were about 2.05×10^{-3}, 1.01×10^5, and 3.03×10^5 Pa, respectively. Corresponding to annealing pressure, the annealed samples were denoted as S1, S2, and S3, respectively.

Structures of the films were characterized by a D/max-RA X-ray diffractometer (XRD) (Rigaku International Corp., Japan) with CuKα radiation, and all the diffraction peaks were calibrated by the (006) diffraction peak of the Al_2O_3 at 41.68°. A Hitachi S4800 energy dispersive spectroscopy (EDS) was used to determine the elements content in the MgZnO films, and the acceleration voltage and magnification of EDS were 15 kV and 5000, respectively. All of the samples were measured at three different locations on the samples surface and the elements contents in the films were determined by using the normalization method after each measurement. The standardless quantification routine was used and performed by hitting the "Quant" button in the main panel. ZAF correction (atomic number, absorption, and fluorescence corrections) was used for calculation. The level of accuracy was 0.1%. Except Mg, Zn, and O, the signal from Al (comes from Al_2O_3 substrate) was also observed. Using the ratio of Al/O = 2/3, the measured oxygen content was subtracted by 1.5 times of the measured Al content. Then, the actual oxygen content in the films can be obtained. The calculated Mg content was about 11.1, 9.3, 7.9, and 3.9% in the as-grown MgZnO film, S1, S2, and S3, respectively. The relative error was less than 10%. The room temperature absorbance measurement was performed using an UV–visible-near infrared spectrophotometer (Shimadzu). Photoluminescence (PL) measurements were performed by the excitation from a 325 nm He–Cd laser with 50 mW power. Electrical properties of the films were measured in Van der Pauw configuration by a Hall analyzer (Lakeshore7707) at room temperature.

Results and discussion

The electrical properties of the as-grown and annealed MgZnO films are listed in Table 1. It shows that the electron concentration of the S1 and S2 is two and three orders of magnitude larger than that of the as-grown MgZnO films, respectively. However, a reproducible p-type conduction of S3 with hole concentration of 4.71×10^{15} cm^{-3} was obtained. It should be stressed that this p-type undoped MgZnO films were obtained under post-annealing processing, that is different from the results reported previously, which show that the undoped p-type MgZnO films were obtained by controlling Mg content in MgZnO films [22].

EDS, XRD, and PL measurements were carried out for explaining the conductive mechanisms of the annealed MgZnO films. EDS measurement shows that oxygen content was about 46.22% for the as-grown films and decreased to 44.34% for S1, but increased to 55.77% for S3. It is well known that the vapor pressure of oxygen was larger than that of Zn and Mg. Furthermore, the vapor pressure of the chemical elements can be changed by

Table 1 Electrical properties of the as-grown MgZnO film and the films annealed at different pressures

Sample	Resistivity (ohm cm)	Carrier concentration (cm^{-3})	Hall mobility (cm^2/(V s))	Conduction type
As-grown	675.0	5.04E + 15	2.11	n
S1	0.7	1.85E + 18	4.95	n
S2	17.4	4.45E + 17	0.93	n
S3	1194.0	4.71E + 15	1.15	p

S1 denotes the sample annealed at 2.05×10^{-3} Pa, *S2* denotes the sample annealed at 1.01×10^5 Pa, and *S3* denotes the sample annealed at 3.03×10^5 Pa

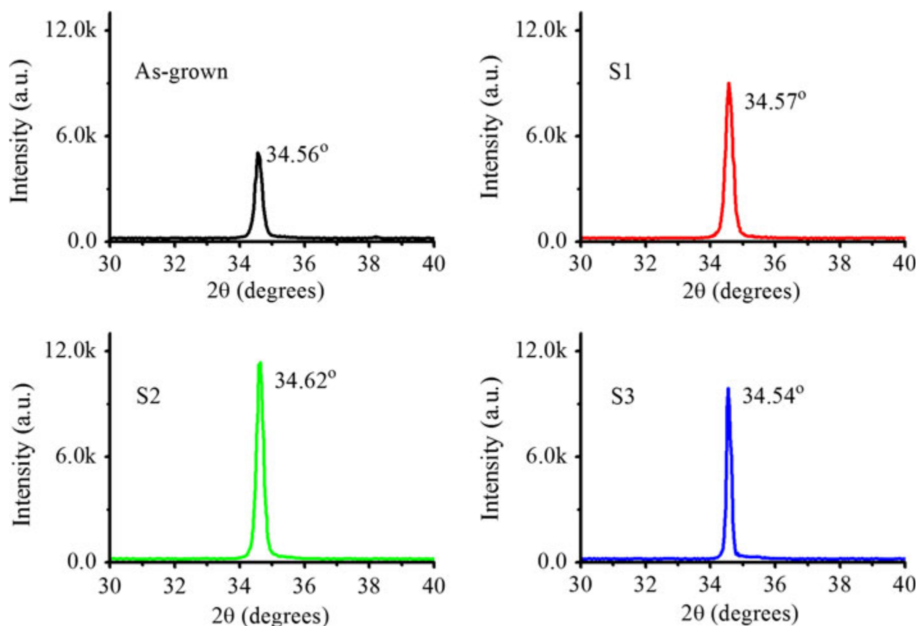

Fig. 1 X-ray diffraction patterns of the as-grown MgZnO film as well as the films annealed at different pressures

adjusting ambient pressure. Therefore, the decreases/increases of oxygen content in S1/S3 can be attributed to the outdiffusion/indiffusion of oxygen in the MgZnO films annealed at different ambient pressure.

Figure 1 shows the XRD patterns of the as-grown and annealed MgZnO films. It shows that only (002) diffraction peak is observed between 34.54° and 34.62° for all the films, indicating that all of the MgZnO films were of single wurtzite structure with (002) preferential orientation. As shown in Fig. 2, the full width at half maximums (FWHM) of the (002) diffraction peak decreases with increasing annealing pressure. This suggests that annealing pressure play an important role in the improvement of the crystalline quality of the films. It is worth noticing that diffraction angle (2θ) of (002) peak increases with increasing annealing pressure while pressure lower than 1.01×10^5 Pa, however, 2θ decreases to 34.54° while annealed at 3.03×10^5 Pa. Since the MgZnO films used in our experiment have a thickness of 1,000 nm, MgZnO films suffer a compressive stress in *c*-axis direction mainly due to thermal stress [27]. If this compressive stress in *c*-axis direction is partly relaxed upon annealing, the decreases of 2θ should be observed. Therefore, increasing in 2θ is not related to stress relaxation. It is well known that there are lots of intrinsic defects in films, such as oxygen vacancy (V_O), zinc vacancy (V_{Zn}), interstitial zinc (Zn_i), interstitial oxygen (O_i), etc. [28–31]. During annealing, the variation of these defects with the oxygen pressure (pO_2) can be expressed as the following:

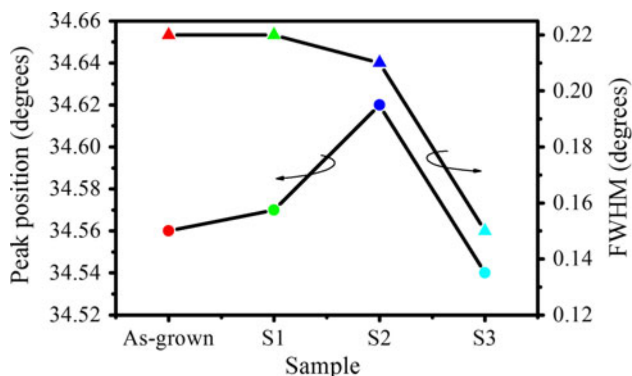

Fig. 2 A plot for variations of position and FWHM of the (002) diffraction peaks of the as-grown MgZnO film as well as the films annealed at different pressures

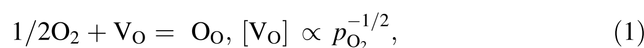

$$1/2\mathrm{O}_2 + \mathrm{V_O} = \mathrm{O_O},\ [\mathrm{V_O}] \propto p_{\mathrm{O}_2}^{-1/2}, \tag{1}$$

$$1/2\mathrm{O}_2 = \mathrm{O_i},\ [\mathrm{O_i}] \propto p_{\mathrm{O}_2}^{1/2}, \tag{2}$$

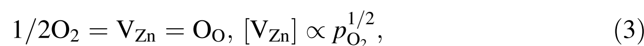

$$1/2\mathrm{O}_2 = \mathrm{V_{Zn}} = \mathrm{O_O},\ [\mathrm{V_{Zn}}] \propto p_{\mathrm{O}_2}^{1/2}, \tag{3}$$

$$1/2\mathrm{O}_2 + \mathrm{V_{Zn}} = \mathrm{O_{Zn}},[\mathrm{O_{Zn}}] \propto p_{\mathrm{O}_2}^{1/2}[\mathrm{V_{Zn}}], \tag{4}$$

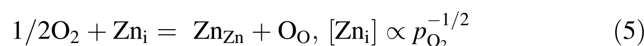

$$1/2\mathrm{O}_2 + \mathrm{Zn_i} = \mathrm{Zn_{Zn}} + \mathrm{O_O},\ [\mathrm{Zn_i}] \propto p_{\mathrm{O}_2}^{-1/2} \tag{5}$$

Here, $[V_O]$ and $[V_{Zn}]$ are the concentrations of the vacancies of oxygen and zinc, respectively. $[Zn_i]$, $[O_i]$, and $[O_{Zn}]$ are the concentrations of the interstitial zinc (Zn_i), interstitial oxygen (O_i), and antisite oxygen (O_{Zn}), respectively. Equations 2 and 3 indicate that concentrations of the O_i and V_{Zn} ought to increase with increasing oxygen pressure. Since the O_i atoms in ZnO films located between O^{2-} and Zn^{2+} layers, the *c*-axis lattice constant will be increased. According to the changes of oxygen content in the annealed films, the increases/decreases of 2θ for S1/S3 was

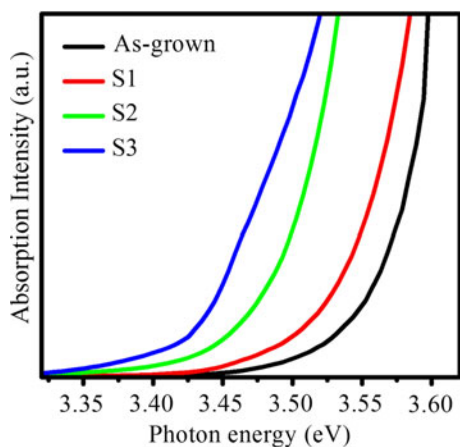

Fig. 3 Room-temperature absorption spectra of the as-grown MgZnO films and the films annealed at different pressures

attributed to the outdiffusion/indiffusion of oxygen in the annealed films, which is consistent with the results of EDS measurement.

Figure 3 shows the room temperature absorption spectra of the as-grown and annealed MgZnO films. Comparing with ZnO [32], the absorption edge of the MgZnO films shift to the higher energy side, this indicates that Mg was incorporated into ZnO films. By increasing annealing pressure, the absorption edge shifts to the lower energy side. By fitting $(\alpha h\nu)^2$ versus $h\nu$ plot shown in Fig. 3 with the relationship of $(\alpha h\nu)^2 \propto (h\nu - E_g)$ (where α is the absorption coefficient, $h\nu$ the photon energy, and E_g the optical band gap), the E_g is estimated to be 3.59 eV for the as-grown MgZnO film and 3.54, 3.49, and 3.44 eV for S1, S2, and S3, respectively. EDS measurement indicates that the ratio of Mg/Zn in MgZnO films decreases with increasing annealing pressure, indicating that the red-shift of the absorption edge can be attributed to the decrease of the ratio of Mg/Zn in MgZnO films by increasing annealing pressure. Since as-grown MgZnO films show n-type conduction, it means that many donorlike defects exist in the as-grown films. The Zn atoms might be incorporated at interstitial sites or/and grain boundaries and act as donor. The decrease of optical band gap can be attributed to the decrease of the ratio of Mg/Zn for Zn atoms being induced to the lattice points upon annealing.

The optical properties of the as-grown and annealed MgZnO films were investigated by PL spectra at room temperature, as shown in Fig. 4. There are two obvious emission peaks for the as-grown and annealed MgZnO films. One is strong spontaneous emission peak in ultraviolet (UV) region, which originates from a near-band-edge (NBE) transition of wide band gap of MgZnO films, namely the recombination of free excitions. The other is defects related visible light (VL) emission band in the range of 2.0–2.6 eV. By comparison, two obvious interesting changes were found from the PL spectra of the as-grown and annealed MgZnO films: (i) the location of the emission peak in the UV region shift toward lower energy side with increasing annealing pressure, which is consistent with the results of absorption spectra measurement; and (ii)

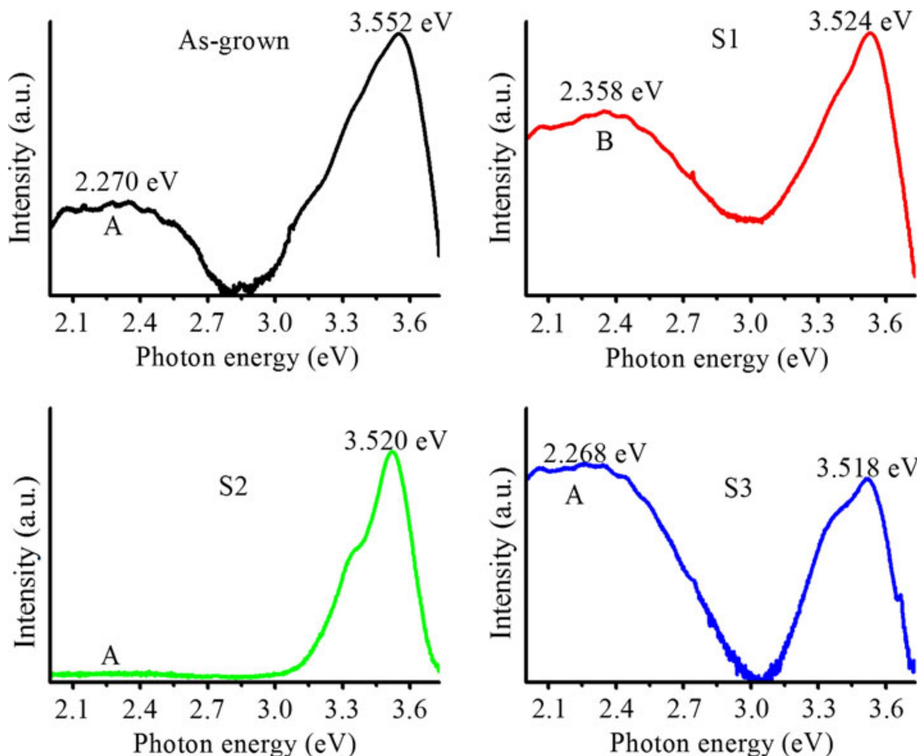

Fig. 4 Room-temperature PL spectra of the as-grown MgZnO film and the films annealed at different pressures

the intensity of the emission peak at 2.270 eV (denoted as band A) increases for S3 and decreases for S2. Moreover, the band A disappears and a new emission peak located at 2.358 eV (denoted as band B) was observed for S1.

From Table 1, it can be found that carrier concentration decreases with increasing intensity of the band A, but increases with increasing intensity of the band B. From the EDS measurement, it was found that the intensity of the band A increases with increasing oxygen content in the annealed MgZnO films and the band B appears in the films with low oxygen content. As discussed in EDS and XRD, the increases/decreases of interstitial oxygen contents were obtained for S3/S1. This variation is consistent with the intensity variation of the band A and B we measured in the experiments. Therefore, the band A must be corresponding to acceptors O_i, whose concentration variations conform to the intensity variation of the band A and the oxygen content variation in the annealed MgZnO films. The p-type conduction of the S3 can be attributed to that the O_i acceptor can compensate V_O and Zn_i donor.

Using the full potential linear muffin-tin orbital method, Sun [33] calculated the defects levels in ZnO films. It was found that the energy interval (2.28 eV) from the conduction bottom to the O_i level formed in bandgap nearly consists with the band A observed in our experiment. Therefore, it is further confirmed that the emission band A is related to O_i, which can be fine explain our experiment results of Hall-effect measurements as shown in Table 1. The band B has been reported in literature and associated with acceptors O_{Zn} in the films [34]. Since the intensity of the band B and the electron concentration show increase for S1, it can be concluded that the band B is not related to acceptors O_{Zn} in films. The origin of the band B is still uncertain and further investigations should be carried out.

Conclusion

Properties of the undoped n-type MgZnO films were investigated by annealing at different pressures. After annealing at 3.03×10^5 Pa, oxygen content in the annealed films show increases and the films transforms into p-type conduction. However, decreasing in oxygen content and increasing in electron concentration were obtained by annealing the films at 1.01×10^5 or 2.05×10^{-3} Pa. The conductivity of the annealed MgZnO films is related to the intensity of the emission peak located at 2.270 eV. Increasing in the intensity of this emission peak results from the increases of the acceptor defect O_i, which compensate the n-type doping effect of Zn_i or V_O and lead to the transition of the conduction type of MgZnO films. This explains why the MgZnO films annealed at 3.03×10^5 Pa show p-type conduction and have a strong emission peak located at 2.270 eV. Form above discussion, it can be concluded that annealing using different pressures can modulate the intrinsic defects in MgZnO films and may be benefit to p-type doping in MgZnO films for device applications.

Acknowledgement This work is supported by the Key Project of the National Natural Science Foundation of China under grant no. 50532050; The Knowledge Innovation Program of the Chinese Academy of Sciences (NO.KJCX3.SYW.W01); The National Natural Science Foundation of China (Nos. 60776011, 60806002 and 10874178). The authors would like to thank Dr. H. F Zhao for useful discussions and advice. The authors also would like to acknowledge financial support through Swedish Research Links via VR.

References

1. Tang ZK, Wong GKL, Yu P (1998) Appl Phys Lett 72:3270
2. Wong EM, Searson PC (1999) Appl Phys Lett 7:2939
3. Kawasaki M, Ohtomo A, Ohkubo I, Koinuma H, Tang ZK, Yu P, Wang GKL, Zhang BP, Segawa Y (1998) Mater Sci Eng B 56:239
4. Bagnall DM, Chen YF, Zhu Z, Yao T, Koyama S, Shen MY, Goto T (1997) Appl Phys Lett 70:2230
5. Iwata K, Fons P, Yamada A, Matsubara K, Niki S (2000) J Cryst Growth 209:526
6. Reynolds DC, Look DC, Jogai B (1996) Solid State Commun 99:873
7. Vispute RD, Talyansky V, Choopun S, Downes M, Sharma RP, Venkatesan T, Wood MC, Lareau RT, Jones KA, Iliadis AA (1997) Appl Phys Lett 70:2735
8. Look DC (2001) Mater Sci Eng B 80:383
9. Narayan J, Dovidenko K, Sharma AK, Oktyabrsky S (1998) J Appl Phys 84:2597
10. Vispute RD, Talyansky V, Choopun S, Sharma RP, Venkatesan T, He M, Tang X, Halpern JB, Spencer MG, Li YX, Salamanca-Riba LG, Iliadis AA, Jones KA (1998) Appl Phys Lett 73:348
11. Ohtomo A, Kawasaki M, Koida T, Masubuchi K, Koinuma H, Sakurai Y, Yoshida Y, Yasuda T, Segawa Y (1998) Appl Phys Lett 72:2466
12. Sun JW, Lu YM, Liu YC, Shen DZ, Zhang ZZ, Li BH, Zhang JY, Yao B, Zhao DX, Fan XW (2007) J Phys D Appl Phys 40:6541
13. Ghosh R, Basak D (2007) J Mater Sci Mater Electron 18:S141
14. Kang SW, Kim YY, Ahn CH, Mohanta SK, Cho HK (2008) J Mater Sci Mater Electron 19:755
15. Ghosh R, Mridha S, Basak D (2009) J Mater Sci Mater Electron 20:S371
16. Minegishi, Koiwai Y, Kikuchi Y, Yano K, Kasuga M, Shimizu A (1997) Jpn J Appl Phys 36:1453
17. Wei ZP, Yao B, Zhang ZZ, Lu YM, Shen DZ, Li BH, Wang XH, Zhang JY, Zhao DX, Fan XW, Tang ZK (2006) Appl Phys Lett 89:102104
18. Yao B, Xie YP, Cong CX, Zhao HJ, Sui YR, Yang T, He Q (2009) J Phys D Appl Phys 42:015407
19. Wang P, Chen NF, Yin ZG, Dai RX, Bai YM (2006) Appl Phys Lett 86:202102
20. Qiu MX, Ye ZZ, He HP, Zhang YZ, Gu XQ, Zhu LP, Zhao BH (2007) Appl Phys Lett 90:182116
21. Shi ZL, Liu DL, Yan XL, Gao ZM, Bai SY (2008) Microelectron J 39:1583
22. Li YF, Yao B, Lu YM, Wei ZP, Gai YQ, Zheng CJ, Zhang ZZ, Li BH, Shen DZ, Fan XW, Tang ZK (2007) Appl Phys Lett 91:232115

23. Zhang X, Li XM, Chen TL, Zhang CY, Yu WD (2005) Appl Phys Lett 87:092101
24. Xiong G, Wilkinson J, Mischuck B, Tüzemen S, Ucer KB, Williams RT (2002) Appl Phys Lett 80:1195
25. Zeng YJ, Ye ZZ, Xu WZ, Lu JG, He HP, Zhu LP, Zhao BH, Che Y, Zhang SB (2006) Appl Phys Lett 8:262103
26. Choopun S, Vispute RD, Noch W, Balsamo A, Sharma RP, Venkatesan T, Iliadis A, Look DC (2006) Appl Phys Lett 75:3947
27. Park SH, Hanada T, Oh DC, Minegishi T, Goto H, Fujimoto G, Park JS, Im IH, Chang JH, Cho MW, Yao T (2007) Appl Phys Lett 91:231904
28. Bylander EG (1978) J Appl Phys 49:1188
29. Vanheusden K, Seager CH, Warren WL, Tallant DR, Voiget JA (1996) Appl Phys Lett 68:403
30. Liu M, Kitai AH, Mascher P (1992) J Lumin 54:35
31. Bo FH, Yan YS, Feng ZP, Yuan WH, Lin LX, Mei C, Sheng ZQ, Hai CY, Guo WZ (2007) Chin Phys Lett 24:2108
32. Ahn K-S, Deutsch T, Yan YF, Jiang C-S, Perkins CL, Turner J, Al-Jassim M (2007) J Appl Phys 102:023517
33. SunYM (2000) PhD thesis, University of Science and Technology of China, July 2000
34. Lin BX, Fu ZX, Jia YB, Liao GH (2001) J Electrochem Soc 144:G110